

# Comparison of Excitatory Currents Activated by Different Transmitters on Crustacean Muscle

## *I. Acetylcholine-activated Channels*

CHRIS LINGLE and ANTHONY AUERBACH

From the Department of Biology, Brandeis University, Waltham, Massachusetts 02254; and the Laboratory of Neurobiology, University of Puerto Rico School of Medicine, San Juan, Puerto Rico

**ABSTRACT** The properties of acetylcholine-activated excitatory currents on the gml muscle of three marine decapod crustaceans, the spiny lobsters *Panulirus argus* and *interruptus*, and the crab *Cancer borealis*, were examined using either noise analysis, analysis of synaptic current decays, or analysis of the voltage dependence of ionophoretically activated cholinergic conductance increases. The apparent mean channel open time ( $\tau_n$ ) obtained from noise analysis at  $-80$  mV and  $12^\circ\text{C}$  was  $\sim 13$  ms;  $\tau_n$  was prolonged e-fold for about every 100-mV hyperpolarization in membrane potential;  $\tau_n$  was prolonged e-fold for every  $10^\circ\text{C}$  decrease in temperature.  $\gamma$ , the single-channel conductance, at  $12^\circ\text{C}$  was  $\sim 18$  pS and was not affected by voltage;  $\gamma$  was increased  $\sim 2.5$ -fold for every  $10^\circ\text{C}$  increase in temperature. Synaptic currents decayed with a single exponential time course, and at  $-80$  mV and  $12^\circ\text{C}$ , the time constant of decay of synaptic currents,  $\tau_{\text{ejc}}$ , was  $\sim 14$ – $15$  ms and was prolonged e-fold about every 140-mV hyperpolarization;  $\tau_{\text{ejc}}$  was prolonged about e-fold for every  $10^\circ\text{C}$  decrease in temperature. The voltage dependence of the amplitude of steady-state cholinergic currents suggests that the total conductance increase produced by cholinergic agonists is increased with hyperpolarization. Compared with glutamate channels found on similar decapod muscles (see the following article), the acetylcholine channels stay open longer, conduct ions more slowly, and are more sensitive to changes in the membrane potential.

### INTRODUCTION

The nature of the molecular events underlying the conductance changes activated by transmitter agents has been vigorously studied in recent years through the use of such techniques as current fluctuation analysis (Anderson and Stevens, 1973), synaptic current analysis (Magleby and Stevens, 1972),

Address reprint requests to Dr. Chris Lingle, Dept. of Biological Sciences, The Florida State University, Tallahassee, FL 32306. Dr. Auerbach's present address is Dept. of Biophysical Sciences, State University of New York, Buffalo, NY 14214.

voltage jumps (Adams, 1977), and most dramatically, the patch clamp (Neher and Sakmann, 1976). Much of this work has been done on a few specific preparations, primarily the acetylcholine (ACh)-gated channel of the frog (Katz and Miledi, 1972; Magleby and Stevens, 1972; Anderson and Stevens, 1973; Neher and Sakmann, 1976; Colquhoun and Sakmann, 1981), the depolarizing ACh channel of *Aplysia* (Ascher et al., 1978), and glutamate- and  $\gamma$ -aminobutyric acid (GABA)-activated channels of arthropods (Anderson et al., 1978; Crawford and McBurney, 1976; Dudel, 1974, 1977, 1978; Dudel et al., 1977; Cull-Candy and Parker, 1982; Cull-Candy et al., 1981; Onodera and Takeuchi, 1975, 1978). At a simple level, the basic kinetic aspects of channel activation by transmitters appear remarkably similar among various types of channels. This apparent similarity stems largely from the success of the del Castillo and Katz (1957) model of receptor activation in accounting for both steady-state and kinetic aspects of macroscopic current measurements. However, the physical events associated with the gating and permeation processes of ionic channels remain poorly understood and it is not yet entirely clear to what extent aspects of channel function may be generalizable to all transmitter-gated channels. Since much of our knowledge concerning channels is based on only a few principal preparations, it is difficult to generalize about some aspects of channel function. For example, glutamate channels have been studied mostly in arthropods, whereas ACh excitatory channels have been most extensively studied in vertebrate preparations and *Aplysia*.

The present paper is part of our attempt to address these issues by comparing the properties of ACh-gated excitatory currents and glutamate-gated excitatory currents found within the same organism (Marder, 1976; Lingle, 1980). Suitable preparations for such an investigation are the muscles of the decapod crustacean foregut. In the spiny lobster *Panulirus interruptus*, some of the striated muscles of the foregut receive cholinergic excitatory innervation (Marder, 1976; Lingle, 1980), whereas other muscles receive a glutamatergic innervation (Lingle, 1980). In addition, a third group of muscles receives a glutamatergic innervation while also displaying ACh receptors extrajunctionally (Lingle, 1980). These muscles are anatomically and physiologically similar to other crustacean striated muscles (Govind et al., 1975). The basic pharmacological properties of the cholinergic and glutamatergic responses have been presented elsewhere (Marder and Paupardin-Tritsch, 1980; Lingle, 1980; Lingle et al., 1981). In the present paper the properties of excitatory ACh-gated currents on the gm1 muscle of lobster and crab are examined. In the following paper (Lingle and Auerbach, 1983), aspects of both excitatory glutamate-gated and ACh-gated currents on the gm6 muscle of the same species are studied and a comparison of the two types of excitatory currents is made.

The results of this study show that within the experimental limitations imposed by these crustacean preparations, the processes determining excitatory current kinetics and ion conductance of ACh-gated channels in marine decapod Crustacea appear in many ways to be similar to cholinergic channel properties in other phyla and are distinct from the properties of glutamate

channels found in arthropods. An abstract describing some of these findings has been published (Lingle and Auerbach, 1980).

#### MATERIALS AND METHODS

##### *Animals and Preparations*

Experiments described in this paper were performed on the gm1 muscle of spiny lobsters, either *Panulirus interruptus* or *Panulirus argus*, or on the gm1 muscle of the crab *Cancer borealis*. The gm1 muscle and others in the decapod foregut are striated muscles similar anatomically and physiologically to the striated muscles of the decapod abdomen and appendages (Govind et al., 1975). The gm1 muscle receives innervation from four identifiable cholinergic excitatory motor nerves (Marder, 1976; Marder and Paupardin-Tritsch, 1980). No inhibitory innervation to this muscle has been described. *P. interruptus* were obtained from Pacific Biomarine, Venice, CA, and maintained at 12–15°C in instant ocean aquaria until use. *P. argus* were caught off Puerto Rico and maintained in outdoor running seawater. *C. borealis* were obtained from local Boston markets and maintained at 4°C.

Muscles with attached nerves were isolated after removal of the stomach by dissection through the dorsal carapace and maintained in a physiological saline made up of (mM): for *Panulirus*, 479 NaCl; 12.7 KCl; 13.7 CaCl<sub>2</sub>; 3.9 MgSO<sub>4</sub>; 8.3 Tris base; and 3.6 maleic acid; and for *Cancer*, 440 NaCl; 11 KCl; 9.8 CaCl<sub>2</sub>; 26 MgSO<sub>4</sub>; 11 Tris base; and 4.8 maleic acid. When necessary, the pH was adjusted from 7.3 to 7.5. In some experiments, 5 or 20 mM MnCl<sub>2</sub> or 5 mM CsCl was included in the saline. This served to increase muscle fiber membrane resistance and to enhance the stability of electrode penetrations during depolarization or agonist application.

Muscles were pinned in 1–3-ml perfusion chambers and superfused continuously with saline. The temperature of the saline was controlled by a Peltier (Cambion, Cambridge, MA) thermoelectric device. Agonists were applied to the muscle surface by standard procedures (1 M ACh; 0.1 M carbamylcholine) using a floating-ground iontophoretic circuit. Iontophoretic current was monitored with a virtual ground current monitor.

##### *Analysis of Agonist-induced Current Fluctuations*

For noise analysis, regions of muscle fibers were clamped with a standard two-microelectrode technique using 2–5-M $\Omega$  electrodes filled with 3 M KCl. As a result of the large diameter (100–250  $\mu$ m) of these crustacean muscle fibers and the low input resistance (0.2 M $\Omega$ ) of the fibers, only a small region of the fiber could be considered to be clamped over the necessary frequency range (see Finger and Stettmeier, 1980). As a result, care was taken to position the ACh-containing pipette immediately between the two intracellular electrodes all within an area of  $\sim$ 100  $\mu$ m diam. The attempt to clamp these cholinergic currents successfully may have been aided by the distribution of cholinergic receptors on this muscle. Although the precise distribution of receptors is not known, cholinergic currents can be elicited at virtually any position on the muscle. Thus, it is likely that under the present voltage-clamp conditions, a large fraction of ACh-activated currents result from channels in an area immediately between the clamp electrodes. Possible sources of error in the measurements are considered in the Results. Agonist-activated currents (up to 150 nA) were generated by iontophoretic application and stored on magnetic tape. In general, at least 15 s of stable agonist-activated currents were recorded. High-gain records of 0.1 Hz AC-coupled current noise were subsequently digitized by a PDP-12 computer (Digital

Equipment Corp., Maynard, MA) at 500 or 1,000 Hz after low-pass-filtering at 250 or 500 Hz (four-pole Butterworth), respectively. The digitized data were screened, and blocks that contained obvious artifacts were rejected. 1,024-point blocks of data were cosine-tapered and then transformed via an FFT. 10–20 spectra from such 1,024-point blocks were then averaged. Spectra from an equal number of blocks obtained from membrane current noise in the absence of agonist were subtracted from the spectra obtained with agonist. The variance of the drug-activated noise was only about one to two orders of magnitude greater than the background noise. The zero-frequency asymptote and the cutoff frequency of the difference spectra were determined by alignment by eye of a computer-generated single Lorentzian superimposed on the data points. No attempt to account for high-frequency deviations from a single Lorentzian with other spectral components was made. The time constant of the process underlying the power spectrum was obtained from  $\tau = 1/(2\pi f_c)$  where  $f_c$  is the frequency at which the spectral power drops to one-half the maximal power.  $\gamma$  was obtained from the following relationship:  $\gamma = [S(0)\alpha]/2\mu(V - V_{eq})$ , where  $S(0)$  is the zero-frequency asymptote,  $\mu$  is the mean agonist-induced current,  $V$  is the holding potential, and  $\alpha$  is  $1/\tau$ . The reversal potential,  $V_{eq}$ , was assumed to be 0 mV (Marder, 1976; Lingle, 1980, Tables I and II).

#### *Analysis of Synaptic Currents*

Since crustacean muscles receive a distributed innervation, information concerning the time course of synaptic currents can most easily be gained through extracellular focal recording of currents generated at single synaptic regions (Dudel and Kuffler, 1961; Onodera and Takeuchi, 1975). Two saline-filled, fire-polished pipettes with 5–15- $\mu\text{m}$  tip diameters were used to record differentially the extracellular voltage change produced in response to synaptic current flow. In order to locate a synapse, the nerve to the muscle was continuously stimulated at 5–10 Hz (a frequency that usually does not produce muscle contraction), while one extracellular focal pipette was moved along the fiber. When a synaptic area was found, a potential drop corresponding to an outward current was also sometimes apparent in addition to the synaptic inward currents. The time course of this potential is clearly slower than the potential resulting from inward synaptic currents and may reflect current conducted down the fiber from more distant synapses. Thus, after location of a synaptic site, it was important to exclude any possible contamination from the “outward” currents to obtain an accurate approximation of the synaptic currents. To minimize this problem, three different recording configurations of the reference electrode were attempted: (a) mounting the electrode piggy-back on the first electrode; (b) placing it on the membrane of the same muscle fiber at a site adjacent to the first electrode; and (c) placing it at some distance away in the bath. Of these three procedures, localization of the reference electrode just above the focal electrode over the synaptic site seemed to minimize the contribution of currents from sources other than beneath the focal pipette.

Focal currents were recorded either with the membrane potential held by current clamp or by a two-electrode voltage clamp of the synaptic region. The results were essentially identical, since the intracellular voltage change during nerve stimulation at 5 Hz under current-clamp conditions was generally  $<10$  mV even at hyperpolarized potentials. Routinely, the focal pipette was positioned first, followed by insertion of the voltage and current electrodes on opposite sides of the focal pipette, all electrodes being within 100  $\mu\text{m}$ .

Because of the small size of the currents, excitatory junctional currents (ejc's) were stored on tape (FM tape recorder [A. R. Vetter Co., Rebersburg, PA] at 16 ips) and

later digitized (125–500  $\mu\text{s}$ /point) and averaged with a MINC-11 (Digital Equipment Corp.) computer. Baselines were chosen either from the portion of the trace before the synaptic current or after relaxation of the current. After the generation of a semilogarithmic plot, a linear range of the semilog plot was chosen, over which a least-squares regression of the points was calculated in order to calculate a time constant.

#### *Steady-State Current*

To obtain an estimate of the steady-state properties of the agonist-activated currents, agonist was applied iontophoretically to a voltage-clamped region of the muscle fiber. To approximate a steady-state situation, the rise time of the iontophoretic responses was kept at  $>200$  ms. From a consideration of the apparent mean channel open time as obtained from the noise and ejc analyses of this paper, it is likely that the opening and closing processes of the ACh channels are close to steady state for a given iontophoretic dose at the peak of a response. Thus, the voltage dependence of the amplitude of the agonist-activated iontophoretic currents might be expected to provide a reasonable approximation of the voltage dependence of the equilibrium of the channel activation process(es). In order to minimize problems that might lead to slow changes in sensitivity, such as subtle changes in position of the iontophoretic electrode, desensitization, or ionic redistribution, responses at different voltages were usually normalized to control responses obtained at  $-80$  or  $-60$  mV. In such cases, the control responses were obtained both before and after a response at the test potential.

#### *Series Resistance*

No compensation has been made for any voltage drop that may reflect the existence of a resistance in series with the membrane conductances. Although in vertebrate neuromuscular preparations the contribution of a series resistance has proved negligible, that may not be the case for these large, invaginated crustacean muscle fibers. Thus, values for the voltage dependence of any parameter may be expected to underestimate the true voltage dependence. This uncertainty over the actual imposed membrane voltage may also contribute to the large variation in apparent voltage dependence that was observed.

### RESULTS

#### *ACh-activated Currents*

The iontophoretic application of ACh to the surface of gm1 muscle fibers produces mean current increases of up to several hundred nanoamperes. To avoid problems associated with the activation of channels in regions not subject to adequate voltage control, the ACh-containing pipette was always positioned immediately between the two intracellular electrodes, all three within an area of  $\sim 100$   $\mu\text{m}$  diam. By reversing the bucking voltage on the iontophoretic pipette, stable ACh-activated current increases could be generated (Fig. 1A). For noise analysis, currents were generally kept at  $<100$  nA. High-gain AC-coupled records of the ACh-activated currents revealed an increase in current fluctuations (Fig. 1A).  $\text{Mn}^{++}$  or  $\text{Cs}^+$ , when added to the saline, minimized background current fluctuations without modifying the characteristics of agonist-activated fluctuations (Figs. 1A and B and Table I).

The ACh-activated current fluctuations were analyzed as described in Materials and Methods and power spectra of the current fluctuations were

generated. In Fig. 1B, representative spectra of the frequency components of ACh-activated current noise are shown for both normal and manganese-containing saline. Both spectra are fit fairly well with single Lorentzian functions, although some deviation can be seen at the higher frequencies of the spectrum. Such deviations are variable from spectrum to spectrum and

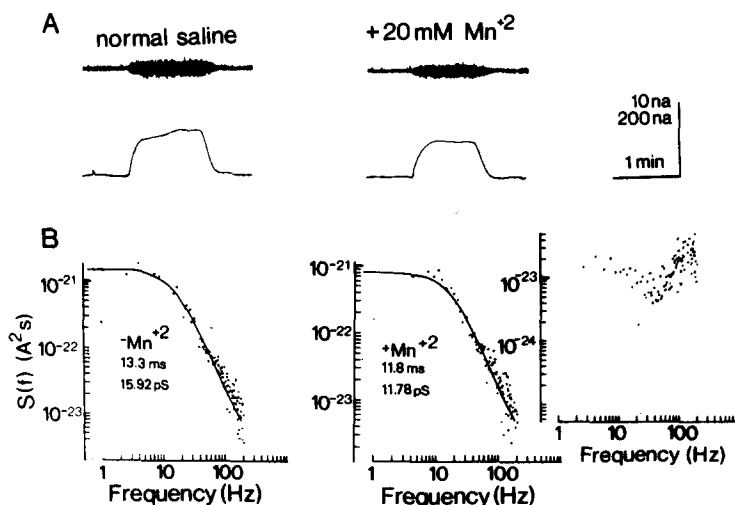


FIGURE 1. (A) ACh-activated membrane currents and current noise on muscle gml of *Panulirus argus*. Each pair of traces shows on the bottom a low-gain DC recording of membrane currents produced by application of ACh to the surface of a gml muscle fiber and on the top a high-gain AC-coupled recording of the same membrane currents. ACh induces a large increase in membrane current noise. Traces were at  $-60$  mV. Right-hand records were from the same muscle in saline containing 20 mM manganese chloride. The AC-coupled signal was digitized at 500 Hz and filtered at 250 Hz for analysis. For purposes of display, the traces were also captured on a chart recorder with effective bandwidth near 100 Hz. Vertical calibration is 200 nA for the DC recording and 10 nA for the AC trace. The horizontal calibration is 1 min. (B) Power spectra of the frequency components of the ACh-activated membrane current noise. Spectra were obtained from the current records at  $-60$  mV shown in Fig. 1A. Each spectrum is the difference between a spectrum of membrane current in the presence of ACh and a similar spectrum of background current noise taken just before ACh application. Membrane potential was  $-60$  mV and temperature was  $12^{\circ}\text{C}$ . Lorentzians were fit by eye. The inset in Fig. 1B shows a spectrum of the background noise used in the generation of the ACh noise spectrum on the right.

could reflect additional spectral components, changes in high-frequency components of background noise during the application of agonist, or the band-pass characteristics of the anti-aliasing filter. Such deviations will not be considered further in this analysis.

Spectra of membrane current noise in the absence of agonist typically showed some gradual diminution in power from DC to  $\sim 100$  Hz with an increase in amplitude at frequencies above 100 Hz (Fig. 1B, inset). Such a

result is consistent with characteristics of background spectra from other preparations (Anderson and Stevens, 1973; Anderson et al., 1978). In general, the amplitudes of background spectra were at least 1.5 an order of magnitude less than the agonist-activated spectra over frequencies up to  $\sim 100$  Hz.

From spectra that are generated by the behavior of discrete ionic channels, two parameters of the elementary units underlying such spectra can be determined. The total amplitude of the power at all frequencies described by a Lorentzian function yields an estimate for the apparent mean amplitude of the elementary units, i.e., the single-channel conductance,  $\gamma$ . Similarly, the cutoff frequency,  $f_c$ , of the single Lorentzian fit to the noise power spectrum

TABLE I  
VALUES OF  $\tau_n$  AND  $\gamma$  FOR ACh-ACTIVATED CURRENTS FROM THE gml  
MUSCLE OF *P. argus*

Fiber	Temper- ature	Mn <sup>++</sup>	n	B(V)	$\tau(0$ mV)	r	$\gamma$
	C						
1	22	±	13	84.8	1.86	0.91	26.9±1.6
	12	±	14	139.3	8.36	0.83	12.4±0.7
2	13	+	5	91.86	4.79	0.57	19.6±0.9
3	23	+	10	115.47	1.69	0.91	47.8±4.2
4	24.5	+	5	85.24	1.11	0.97	54.8±4.9
5	13	-	8	85.4	4.32	0.81	25.0±1.6

Mn<sup>++</sup> indicates whether manganese was included in the saline; n is the number of determinations at a particular site; B(V) is the change in membrane potential necessary for an e-fold change in  $\tau_n$ ;  $\tau(0)$  is the value of  $\tau_n$  in milliseconds extrapolated to 0 mV membrane potential; r is the correlation coefficient for the line drawn through the values of  $\tau$  as a function of membrane potential;  $\gamma$  is the single-channel conductance in pS  $\pm$  SEM.

is used to calculate a predominant mean time constant,  $\tau_{\text{noise}} = \tau_n = 1/(2\pi f_c)$ . We shall consider this an apparent mean channel open time. However, it is important to keep in mind that the interpretation of the physical meaning of the apparent mean open time obtained from noise spectra depends on the particular model of the kinetic processes underlying channel operation (Colquhoun and Hawkes, 1977, 1981; Sakmann and Adams, 1979).

Because of the problems associated with a limited space clamp of these muscle fibers and inadequate information about the density and distribution of the ACh receptors and effective concentration of applied agonist, possible artifactual grounds for the above results must be considered. As one test of the efficacy of the system, the dependence of  $\gamma$  on the magnitude of the mean current increase produced during application of agonist was examined. This is plotted in Fig. 2 for one fiber and shows that at 13°C, even at mean current increases up to 150 nA,  $\gamma$  is fairly constant. At 22°C, at high mean current increases,  $\gamma$  shows a trend toward smaller values. Large mean current increases might be expected to produce underestimates of  $\gamma$  for two reasons. First, with large amounts of agonist, the low concentration limit might be violated (Anderson and Stevens, 1973). Second, large mean current increases may

produce a substantial alteration in the area over which the cell is effectively clamped. If the spectra of ACh-activated current noise in this study reflect only the frequency-dependent filtering by the muscle fiber of current injected through the ACh channels, rather than the spectral characteristics of the channel fluctuations, as the mean current is increased, high-frequency spectral components would be lost and the estimate of  $\gamma$  would become progressively diminished. Because of the constancy of  $\gamma$  as a function of the mean current increase, the problem of high agonist concentration appears minimal. Other arguments in support of the adequacy of these spectra derive from the results presented below.

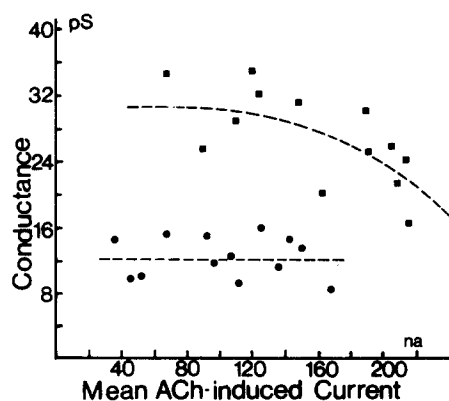


FIGURE 2. Dependence of the single-channel conductance on the magnitude of the mean current increase produced by ACh. All points are from one gm1 fiber. Circles indicate values obtained at 12°C and squares indicate values obtained at 21°C. Lines were fit by eye.

#### *Properties of the Apparent Mean Open Time*

The average value of  $\tau_n$  at  $-80$  mV and 12°C was  $13.1 \pm 1.6$  ms (SEM;  $n = 7$ ) in saline containing 20 mM manganese chloride and  $12.1 \pm 1.9$  ms (SEM;  $n = 3$ ) in normal saline. The characterization of the dependence of apparent mean channel open time on such parameters as voltage or temperature provides information as to the nature of the underlying molecular events associated with channel activation. In all 15 fibers that were examined,  $\tau_n$  was prolonged by hyperpolarization. Considerable variability was observed in the actual magnitude of the voltage dependence, but for the five fibers listed in Table I, on the average an e-fold change in  $\tau_n$  occurred every 100 mV. In Fig. 3A, values for  $\tau_n$  are plotted as a function of membrane potential for the three fibers showing the largest voltage dependence. Because of the similarity in the magnitude of the voltage dependence of  $\tau_n$  in these fibers, the value of 85 mV/e-fold change in  $\tau_n$  may be a more correct approximation of the true voltage dependence.

The effect of temperature on  $\tau_n$  was also examined. Fig. 3 provides a qualitative indication of the effect of temperature in that lower temperatures



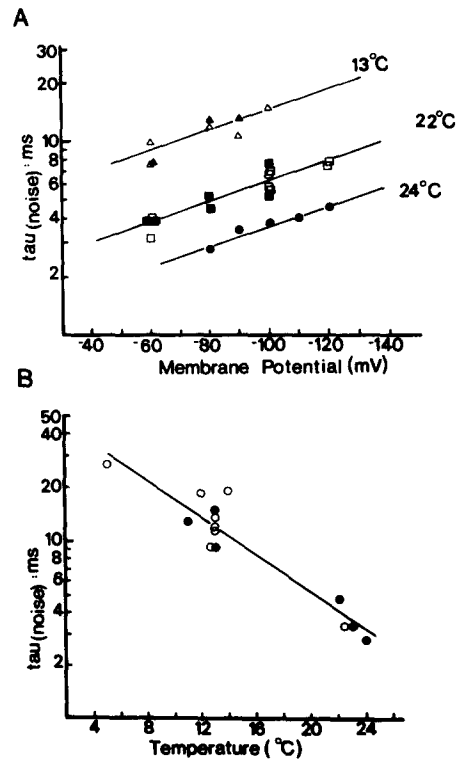


FIGURE 3. (A) Voltage dependence of the cutoff frequency of spectra generated from ACh-induced current noise. Three separate fibers from the gml muscle of *P. argus* are shown at three separate temperatures. Lines are linear regressions to all points both with and without  $Mn^{++}$ . The linear regression for each fiber yielded a slope of 85 mV/e-fold change in  $\tau_n$ . Open symbols were obtained in the presence of 20 mM  $MnCl_2$  and closed symbols were in normal saline. (B) Temperature dependence of  $\tau_n$ . Values of  $\tau_n$  from eight different fibers of the gml muscle of *P. argus* were obtained over the range of 5.5–24°C at –80 mV. The linear regression to the points indicates that  $\tau_n$  changes 3.4-fold for every 10° change in temperature. Open symbols were in the presence of 20 mM  $MnCl_2$ .

prolong the apparent mean open time. The effect of temperature on  $\tau_n$  is plotted in Fig. 3B. For eight cells at –80 mV,  $\tau_n$  was prolonged approximately threefold for a 10° decrease in temperature.

#### *Properties of $\gamma$ , the Apparent Single-Channel Conductance*

The average value of  $\gamma$ , the apparent single-channel conductance, calculated from the integral of the single Lorentzian function fit to each spectrum of ACh-induced current noise, was  $18.2 \pm 3.0$  pS (SEM;  $n = 7$ ) with  $Mn^{++}$  and  $21.0 \pm 5.2$  pS (SEM;  $n = 3$ ) without  $Mn^{++}$  at 12°C and –80 mV. For 15 cells at three different temperatures no dependence of  $\gamma$  on voltage was observed

(Fig. 4A). Within individual fibers there were indications of alterations in  $\gamma$  with membrane potential, but no consistent pattern was observed.

The dependence of  $\gamma$  on temperature is plotted in Fig. 4B for 15 cells. The slope of the regression to these points indicates a  $Q_{10}$  of the apparent mean single-channel conductance of 2.4. Fig. 4B also illustrates data from a single fiber that show the temperature dependence of  $\gamma$  more clearly. The  $Q_{10}$  of conductance from this fiber was 2.6.

It is useful to consider whether the above results concerning the voltage and temperature dependence of  $\tau_n$  and  $\gamma$  could be accounted for simply by alterations in the space clamp produced by voltage or temperature. If the present spectra represented muscle fiber-filtering characteristics (Finger and Stettmeier, 1980), the nonlinearity of the current-voltage relations of crustacean muscle fibers (membrane resistance is substantially reduced as cells are depolarized above resting potential) would lead to an apparent lengthening of  $\tau_n$  and a decrease in  $\gamma$  as the cell was depolarized. Similarly, as the temperatures were increased with a concomitant decrease in membrane resistance, at the higher temperatures,  $\tau_n$  would be expected to become slower and  $\gamma$  would be smaller. These predictions are entirely contrary to the observed trends. If anything, these problems might suggest that in some cases the true values for the voltage and temperature dependence of  $\tau_n$  and  $\gamma$  are underestimated by the present experiments. Two additional points that support the idea that the spectra obtained from ACh-induced current noise in the gm1 muscle are reasonable representations of the frequency components of the underlying channel openings and closings are that (a) spectra of glutamate-induced currents from the gm6 muscle of the lobster foregut have cutoff frequencies at substantially higher values than the spectra of ACh-current fluctuations (Lingle and Auerbach, 1983), and (b) as will be shown below, the time constant of decay of focally recorded synaptic currents on the gm1 muscle of *P. interruptus* and *C. borealis* is similar to the value of  $\tau_n$ .

From the above considerations, the spectral characteristics of current fluctuations around the mean current observed during application of ACh to the gm1 muscle can be considered to directly reflect the predominant kinetic process underlying the openings and closings of the ACh-gated ionic channels.

#### *Properties of Synaptic Currents on the gm1 Muscle*

In most systems, including some arthropod preparations, in which the kinetic properties of the synaptic currents have been compared with the kinetic properties of the ionic channels activated by the appropriate agonist, the apparent mean channel open time has been found to be the primary determinant of the rate of decay of the synaptic currents (Magleby and Stevens, 1972; Anderson and Stevens, 1973; Anderson et al., 1978; Crawford and McBurney, 1976; Dudel et al., 1977; Gardner, 1980; Gardner and Stevens, 1980; Faber and Korn, 1980). We have therefore examined the properties of synaptic currents on the gm1 muscle in order to make a comparison with the characteristics of ACh-induced current noise.

Typical digitized records of the average of at least 60 extracellular focal excitatory junctional potentials (ejc's) are shown in Fig. 5 for a gm1 muscle

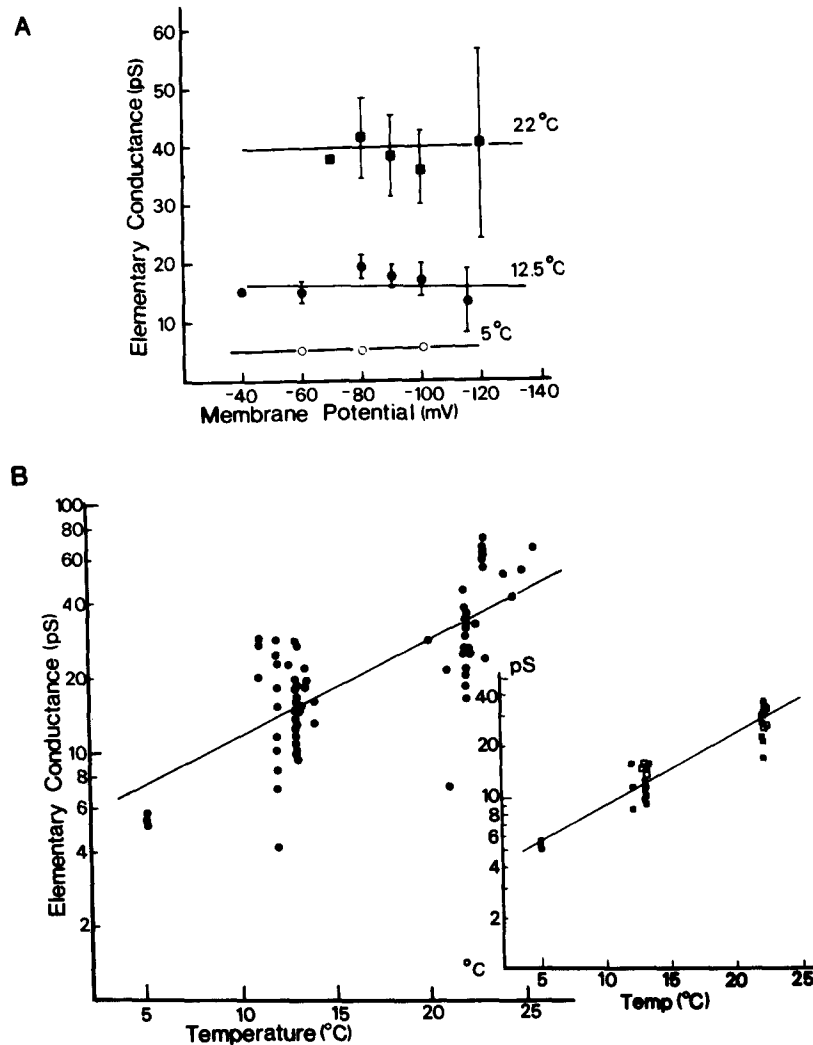


FIGURE 4. (A) Voltage dependence of the single-channel conductance,  $\gamma$ . Values of  $\gamma$  are plotted vs. membrane potential for three different temperature ranges. Points at 22°C include values in the range of 20–24°C; points at 12.5°C include temperatures in the range of 10–14°C. Each point is the mean with error bars indicating SEM.  $\gamma$  was calculated from the power spectra as described in Materials and Methods. (B) Temperature dependence of  $\gamma$ . Values of the single-channel conductance as estimated from power spectra are plotted against temperature. Values were obtained from 15 fibers from the gm1 muscle of *P. argus*. The linear regression to the points indicates that  $\gamma$  increases 2.4-fold for every 10° increase in temperature. The inset shows temperature dependence of  $\gamma$  from a single gm1 fiber. The plot is identical to that in B, but also indicates the lack of effect of  $Mn^{++}$  on conductance. A  $Q_{10}$  of 2.6 was obtained from this fiber. Open symbols were obtained in normal saline, closed symbols with 20 mM  $MnCl_2$ .

from *P. interruptus*. It is likely that the focal pipette is sampling currents activated by ACh released from several nerve terminals, and thus the slow rise time and shape of the peak of the ejc's may reflect the slightly asynchronous release of transmitter from nearby nerve terminals. For synaptic currents on the gml muscle, the time course of the decay phase of the ejc's could be reasonably described by a single exponential function. Semilogarithmic plots

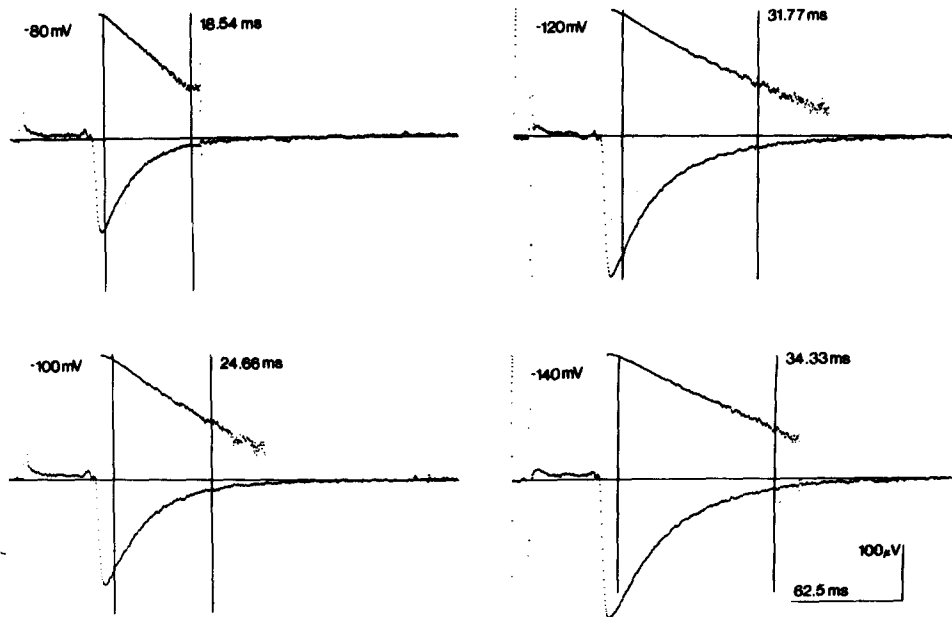


FIGURE 5. Averaged extracellularly recorded excitatory synaptic currents from the gml muscle of *P. interruptus*. At least 60 individual synaptic currents were averaged for each trace. Semilogarithmic plots of the decay phase of the currents are shown above the linear record. A linear regression to the points over the window indicated by the vertical lines was obtained and used to calculate the time constant of the decay process. The membrane potential and value of the time constant were as indicated and the temperature was 10°C.

of the ejc decays with a linear regression fit over a suitable range of the decay process are also shown in Fig. 5. Similar results were obtained from the gml muscle of the crab *Cancer borealis*. For 10 determinations from *Panulirus* at -80 mV and normalized to 12°C ( $Q_{10} = 3.0$ ),  $\tau_{ejc}$  was  $15.1 \pm 1.9$  ms (SEM), whereas for 33 determinations from *Cancer* at -80 mV and 12°C,  $\tau_{ejc}$  was  $13.9 \pm 0.6$  ms (SEM).

As shown in Fig. 5, the time constant of the single exponential ejc decay process was prolonged by hyperpolarization. The results from one fiber in which the membrane potential was repeatedly varied between -60 and -120 mV are shown in Fig. 6A. For all fibers examined (fibers in which the amplitude of the ejc did not extrapolate to a reversal potential within 40 mV of 0 mV were not included in this analysis), the ejc time constant was a simple

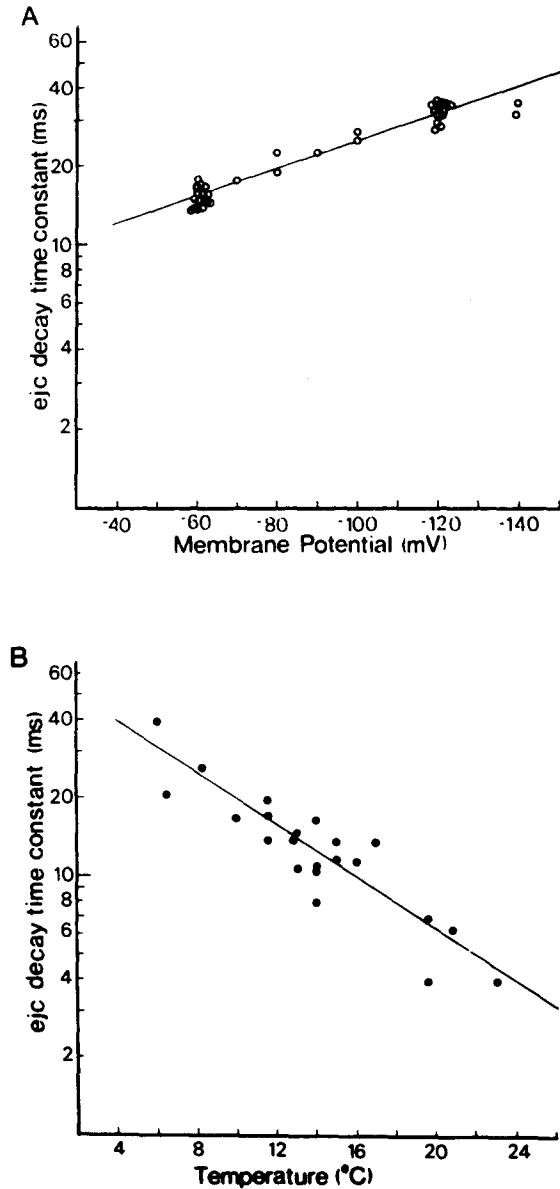


FIGURE 6. (A) Voltage dependence of the time constant of decay of excitatory synaptic currents of the gml muscle of *P. interruptus*. All points are from one fiber. The slope of the linear regression corresponds to an 86 mV/e-fold change in the time constant. The temperature was 10°C. (B) Temperature dependence of the time constant of decay of excitatory cholinergic synaptic currents from the gml muscle of *C. borealis*. All points were from fibers held at membrane potentials in the range of -50 to -70 mV. The linear regression to those points indicates that the time constant of the synaptic current decay is prolonged about threefold for a 10° decrease in temperature.

exponential function of the membrane potential. However, since at most only an 80-mV range was examined, deviations from this simple relationship would be difficult to determine. The linear regression for all points obtained from the fiber of Fig. 6A yielded a voltage dependence for the ejc decay time constant of 86 mV/e-fold change in  $\tau_{\text{ejc}}$ . Table II provides a list of the values of the voltage dependence of  $\tau_{\text{ejc}}$  for other fibers from both *Panulirus* and *Cancer*. As with the results from the analysis of ACh-activated noise, there is considerable variation among fibers. Although the reasons for the variation

TABLE II  
VALUES OF  $\tau_{\text{ejc}}$  AND EXTRAPOLATED REVERSAL POTENTIALS FOR  
CHOLINERGIC SYNAPTIC CURRENTS FROM THE gm1 MUSCLE OF *P. interruptus*  
AND *C. borealis*

Fiber	Voltage range mV	n	Temper- ature C	$\tau(0 \text{ mV})$	$B(V)$	$r$	$V_r$	$r'$
<i>C. borealis</i>								
A202	40-79	(7)	13	5.33	93.8	0.954	+35.7	0.818
A202	36-59	(5)	8.7	11.98	85.0	0.963	+27.3	0.779
S082	50-140	(25)	13.9	4.66	130.1	0.831	+16.8	0.94
A283	40-120	(14)	12.5	7.46	150.4	0.953	+0.3	0.93
S083	60-140	(11)	14.6	4.34	202.8	0.935	-4.6	0.932
0171	40-120	(5)	13.3	8.49	173.5	0.496	+12.4	0.966
<i>P. interruptus</i>								
0211	60-140	(30)	10.0	7.62	86.6	0.965	+37.6	—
M202	80-140	(15)	11.8	6.61	86.1	0.972	-25.3	0.796
M203	80-140	(8)	14.8	6.33	100.9	0.941	-18.9	0.921
M101	80-120	(5)	12.3	7.38	198.4	0.875	+24.4	0.914
M104	70-140		11.5	15.07	148.5	0.927	+35.5	0.850

$\tau(0)$ ,  $B(V)$ , and  $r$  are as in Table I.  $V_r$  is the extrapolated reversal potential of the ejc amplitudes, and  $r'$  is the correlation coefficient of the line through the ejc amplitudes as a function of voltage.

cannot be definitely determined, there are several immediately apparent possibilities. These possibilities include: (a) contamination of ejc currents with currents from adjacent, unclamped fibers; (b) genuine variation in channel kinetics among fibers; or (c) inadequate voltage control of the synaptic region possibly caused by series resistance problems, distance of clamping electrodes from the focal electrode, or positioning of the synaptic site next to a site of electrical coupling with an adjacent muscle fiber. Thus, as with the noise measurements, the voltage dependence of the ejc decay process can be considered a minimal estimation of the true value. As seen in Table II, the mean voltage dependence over the range of about -60 to -140 mV was  $139.3 \pm 22.8$  mV (SEM)/e-fold change in  $\tau_{\text{ejc}}$  for *C. borealis* and  $110.3 \pm 22.5$  mV (SEM)/e-fold change for *P. interruptus*.

$\tau_{\text{ejc}}$  was also prolonged substantially by decreases in temperature. Although the time spent at the peak of the ejc was also prolonged, ejc's at lower temperatures could still be adequately described by single exponential func-

tions over most of the decay phase. For a 10°C decrease in temperature,  $\tau_{ejc}$  was prolonged about threefold for fibers both from *Panulirus* and *Cancer*. This is illustrated in Fig. 6B for fibers from *Cancer* at potentials between -50 and -70 mV.

The amplitude of the peak of the ejc's increased with hyperpolarization in a manner consistent with the increase in the electrochemical gradient for the permeating ions (Fig. 7A). The ejc amplitude varied in a linear fashion with the membrane potential over the limited voltage ranges that could be used. For 11 fibers from Table II, the extrapolated reversal potential from the ejc amplitudes was  $+12.8 \pm 7.0$  mV (SEM).

#### *Steady-State ACh-activated Currents on the gml Muscle*

To obtain qualitative information about the voltage dependence of the steady-state currents activated by cholinergic agonists on the gml muscle, a comparison of the amplitudes of iontophoretic responses of slow rise time (>200 ms) was used. The results from the noise analysis experiments and from the analysis of the synaptic current decays indicate that the rates of the processes involved in channel activation are sufficiently fast that during a slow iontophoretic response at the peak of the response the opening and closing of channels by a particular dose of agonist should approximate a steady-state condition. The use of slow iontophoretic application of unknown amounts of agonist to approximate a steady-state situation was necessary, since the distribution of receptors all along the surface of the gml muscle fibers precludes a meaningful clamp of currents elicited by bath application of agonist.

The amplitude of the cholinergic currents was found to increase in a nonlinear fashion with hyperpolarization (Fig. 7B). This type of result was obtained from *P. argus*, *P. interruptus*, and *C. borealis*. Thus, in contrast to the amplitude of the ejc's (Fig. 7A), the increase in amplitude of the responses to iontophoretic application of ACh cannot be explained solely on the basis of the increased driving force, but suggests that the probability of a channel being open is increased with hyperpolarization.

The use of either ACh or carbamylcholine as agonist produced essentially identical results. As with the noise experiments and the ejc experiments, the magnitude of the voltage dependence of the conductance change produced by iontophoretic application of cholinergic agonist may be an underestimate of the true voltage dependence. First, the imposed membrane potential may overestimate the actual membrane potential at the site of the cholinergic currents. Second, despite the slow time course of the iontophoretic responses, the peak may not totally reflect a steady-state situation, thus diminishing the contribution of the voltage dependence of the closing rate to the overall equilibrium. Third, at frog endplates, the use of high agonist concentrations leads to lowered voltage sensitivity in steady-state current-voltage relations (Adams and Sakmann, 1978). Fourth, desensitization processes might also be expected to contribute to the steady-state currents observed by this method. Since desensitization is markedly increased by hyperpolarization in this prep-

aration (C. Lingle, unpublished observations), this would tend to diminish the magnitude of the voltage dependence that we observed. In addition, this effect of desensitization would lead to exceedingly positive estimates of the reversal potential extrapolated from such currents. In fact, such extrapolated reversal potentials were generally in the range of +20 to +100 mV, as determined by the best correlation coefficient for the relationship,  $g = g(0)e^{AV}$ ,

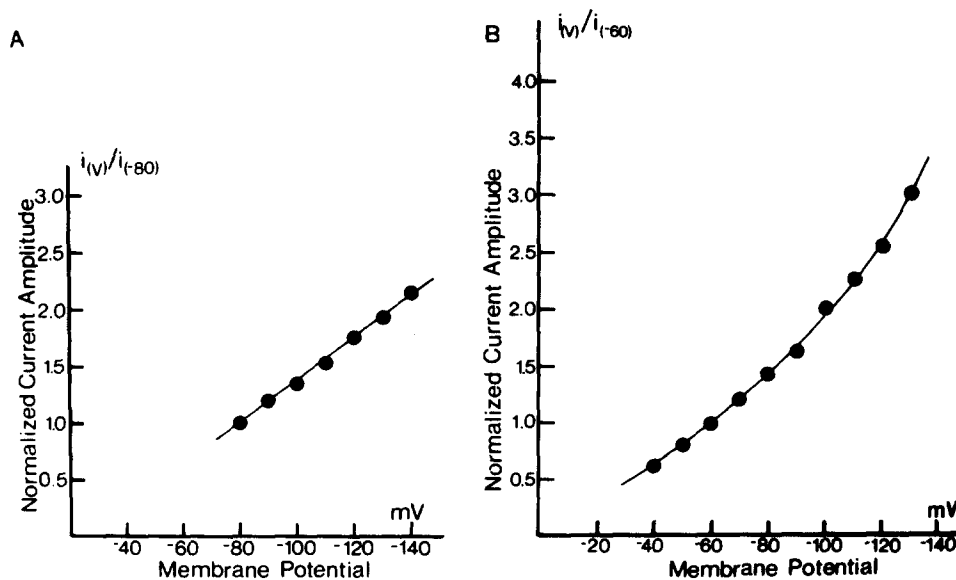


FIGURE 7. (A) Voltage dependence of the amplitude of excitatory cholinergic currents on the gml muscle of *P. interruptus*. The ordinate indicates the magnitude of the potential change recorded extracellularly at a synaptic region to response to stimulation of the motor neurons to the muscle. Each point is the mean of at least three sets of over 60 averaged responses. Responses were normalized to the mean response at  $-80$  mV. (B) Voltage dependence of the amplitude of iontophoretically activated cholinergic currents on the gml muscle of *P. interruptus*. The ordinate indicates the current magnitude expressed as a fraction of the current response at  $-60$  mV. Test responses at  $-60$  mV were obtained immediately before and after each response at potentials other than  $-60$  mV. Each point is the mean of at least three applications at a given potential and SEM are smaller than the points.

where  $V = V_m - V_r$  and  $g$  is the conductance calculated from  $i_{ACh}/V$ . Thus, other processes in addition to channel activation may contribute to the voltage dependence of the amplitude of iontophoretic currents. However, the results are consistent with the idea the hyperpolarization increases the probability that a channel will be open in the presence of agonist.

#### *Junctional vs. Nonjunctional Channels*

The question must be addressed as to whether the results arise from a single, homogeneous population of receptors on the gml muscle. As described,



quantitative information concerning the receptor distribution on the gm1 muscle is not available. Based on iontophoretic application of cholinergic agonists, ACh receptors appear to be present over the entire surface of gm1 muscle fibers.

The paucity of synaptic contacts as determined by searches with extracellular focal pipettes indicates that it is extremely unlikely that the pervasive sensitivity to ACh corresponds entirely to the rather numerous occurrences of synaptic contacts by cholinergic neurons. Other work (Lingle, 1980) has shown that the gm6 and some other muscles of the foregut of *P. interruptus* that receive glutamatergic innervation also display ACh receptors diffusely over the muscle fiber surface.

It is therefore likely that during the noise experiments and the pseudo-steady-state current experiments on the gm1 muscle, both junctional and nonjunctional receptors are activated. Thus, in the present experiments, no clear difference in apparent mean open times obtained from noise and synaptic decay measurements was observed. Thus, it would seem that the kinetic characteristics of those channels could not be distinguished from purely junctional channels and could, in fact, be identical.

In one cell of the 15 from which noise data were obtained, there appeared to be a clear indication of a second component to the power spectrum. Similarly, the decays of synaptic currents from one and perhaps two cells were not clearly single exponential functions. Since these were infrequent observations, these phenomena could not be analyzed in detail and may simply have arisen from causes unrelated to channel kinetics. The present experiments then suggest that although both junctional and nonjunctional receptors may be present on the gm1 muscle, there are no differences in the conductance or kinetic properties of these channels at least within the accuracy of these experiments.

## DISCUSSION

### *Summary of Experimental Results*

The experiments of this study were performed on the gm1 muscle of three decapod crustacean species, the spiny lobsters *Panulirus argus* and *interruptus* and the crab *Cancer borealis*. ACh-activated current noise was analyzed on *P. argus*, synaptic currents were analyzed from both *P. interruptus* and *C. borealis*, and the voltage dependence of iontophoretic cholinergic currents was analyzed from all three species. The primary findings are the following.

(a)  $\tau_n$ , the apparent mean channel open time, at  $-80$  mV and  $12^\circ\text{C}$  was  $\sim 13$  ms;  $\tau_n$  was prolonged by hyperpolarization, varying e-fold with an  $\sim 100$ -mV change in membrane potential and was prolonged approximately three-fold for every  $10^\circ\text{C}$  decrease in temperature.

(b)  $\gamma$ , the single-channel conductance, at  $-80$  mV and  $12^\circ\text{C}$  was  $\sim 18$  pS and was not clearly affected by voltage, but was increased  $\sim 2.5$ -fold for every  $10^\circ\text{C}$  increase in temperature.

(c)  $\tau_{\text{ejc}}$ , the time constant of decay of synaptic currents, at  $-80$  mV and

12°C was ~15 ms for *P. interruptus* and 14 ms for *C. borealis*;  $\tau_{ejc}$  was prolonged e-fold for every 124-mV hyperpolarization in *P. interruptus* and e-fold for every 139-mV hyperpolarization for *Cancer*. In both cases,  $\tau_{ejc}$  was prolonged three-fold for every 10° decrease in temperature.

(d) The magnitude of the conductance change produced by cholinergic agonists when applied by iontophoretic methods was increased by hyperpolarization of the membrane potential.

#### *Interpretation of Kinetic Results*

Given the considerable variation in the values obtained, the results indicate a reasonable correspondence in the rate of the decay of synaptic currents and the value of the cutoff frequency for the spectra of ACh-activated current noise. In addition, both the temperature and voltage dependence of  $\tau_n$  and  $\tau_{ejc}$  are similar. Since noise and ejc values were obtained from different *Panulirus* species, it is possible that this correspondence is fortuitous, but this possibility will not be considered further here. As with most other systems in which such a comparison has been made (Magleby and Stevens, 1972; Anderson and Stevens, 1973; Anderson et al., 1978; Crawford and McBurney, 1976; Dudel et al., 1977; Faber and Korn, 1980; Gardner, 1980; Gardner and Stevens, 1980), the process(es) determining the spectral characteristics of agonist-induced noise also appears to determine the time course of the synaptic current decay.

The formulation of Anderson and Stevens (1973) and Magleby and Stevens (1972) interpreted the rate-determining process controlling the power spectra from ACh-activated current fluctuations and the decay of synaptic currents as the closing rate of the ACh channel. Thus, in accordance with the del Castillo and Katz (1957) model of receptor activation, the agonist binding and unbinding rates are considered to be much faster than the postulated conformational changes involved in the transitions of the channel between conducting and nonconducting states. Other interpretations of the apparent mean open time are possible, however (see Sakmann and Adams, 1979). For the case of ACh-activated channels on the gml muscle, in the absence of other data, it remains simplest to relate the time constant of crustacean nicotinic ACh channels to the closing rate. Thus, the temperature and voltage dependencies of apparent mean open time would reflect influences on the rates at which channels close.

#### *Comparison with Excitatory ACh Responses from Other Organisms*

The excitatory actions of ACh at several vertebrate neuromuscular junctions and on some *Aplysia* neurons have been well characterized in terms of the apparent mean channel open times and the conductance of the channels (Magleby and Stevens, 1972; Anderson and Stevens, 1973; reviews by Steinbach, 1980, and Adams, 1981; Ascher et al., 1978). In addition, some information concerning the excitatory nicotinic channels of the frog sympathetic ganglion (MacDermott et al., 1980) and the rat submandibular ganglion (Ascher et al., 1978; Rang, 1981) is available.

Of the multitude of investigations of channel properties it is not entirely clear to what extent the reported differences represent inherent differences in channel properties or limitations of the experimental techniques when applied to particular preparations. Of the vertebrate neuromuscular junction studies, values for mean open time and conductance have been obtained from human, rat, mouse, frog, toad, snake, and chicken preparations (reviewed by Steinbach, 1980). In general, at 20°C the mean open time of junctional ACh receptors from fast-twitch muscles is on the order of 1–3 ms, the single-channel conductance is in the range of 20–25 pS, and values for the voltage dependence of the mean open time reported for junctional receptors are in the range of 85 (frog) to 110 mV (rat) per e-fold change in mean open time. The above parameters of the vertebrate nicotinic neuromuscular junction ACh receptor are similar to those observed for the lobster gml muscle ACh receptor. Although at 20°C the mean channel open time in the lobster is somewhat longer, the values for single-channel conductance and the voltage dependence of the mean channel open time are not too different from the values observed on vertebrate preparations.

Based on the studies of ganglionic nicotinic preparations, a simple picture of the ganglionic channel has not as yet emerged. On amphibian sympathetic ganglia, the decays of nicotinic synaptic currents are described by a single exponential function (Kuba and Nishi, 1979; MacDermott et al., 1980) with, in the latter study, a mean decay time of 5.3 ms at  $-50$  mV and  $\sim 22^\circ\text{C}$ . In both studies the voltage dependence of the decay of the synaptic currents is slight, being  $>250$  mV/e-fold change in the decay rate (MacDermott et al., 1980; Kuba and Nishi, 1979). In contrast, at the rat submandibular ganglion, excitatory synaptic currents and voltage-jump-induced relaxations of ACh currents decay with a bi-exponential time course with a fast component of 5–9 ms and a slow component of 27–45 ms at 20°C and  $-40$  mV (Rang, 1981). Both components are prolonged by hyperpolarization changing e-fold every 100 mV. Spontaneous miniature potentials decayed with a single exponential time course corresponding only to the fast component. The biphasic decays seen in the rat ganglion were interpreted to represent most probably two populations of ACh channels. Neither the frog or rat ganglionic channels appear to be closely analogous to the crustacean ACh channel.

On the gml muscle, only one population of channels was distinguished in the present study, although there are good reasons to think that both junctional and nonjunctional ACh receptors are present on the gml muscle. One trivial reason for not discerning two distinct populations would be that nonjunctional channels represent a small fraction of the total channels activated. However, since ACh currents are easily activated at any position on these muscles, it seems more likely that the similarities between noise and ejc measurements reflects a similarity between junctional and nonjunctional channels. It is possible that the accuracy of these experiments was not sufficient to discern two populations that might differ subtly in kinetic or conductance parameters. However, in the rat submandibular ganglion a fivefold difference in mean open time was observed between the two apparent populations (Rang, 1981).

Such a difference would certainly have been distinguishable in the present experiments.

The substantial differences that are observed among junctional and non-junctional channels on vertebrate neuromuscular preparations are generally based on the examination of nonjunctional channels under conditions of denervation or development. Thus, the nonjunctional receptors of the innervated decapod muscle are not strictly analogous to the nonjunctional receptors of the vertebrate preparations. Although in developing muscles or in muscles undergoing reinnervation two distinct populations of channels can be distinguished (Michler and Sakmann, 1980; Brenner and Sakmann, 1978), the properties of nonjunctional receptors that persist after the stable formation of mature synapses have not been clearly established. In this regard, junctional and nonjunctional ACh channels during development of chick muscle and on in vitro chick muscle cells cultured with spinal neurons show identical mean channel open times (Schuetze, 1980; Schuetze et al., 1978). Thus, on decapod cholinergic foregut muscles the apparent homogeneity in properties of ACh receptors probably comprised of both junctional and nonjunctional receptors is not necessarily at variance with results from the vertebrate neuromuscular preparations.

It has been suggested (Sheridan, 1976; Lester et al., 1978; Dionne and Parsons, 1981) that the magnitude of the voltage dependence of the mean open time of ACh channels may be of possible functional significance in minimizing the shunting effect of synaptic currents during subsequent electrogenic events. This type of explanation would suggest that these crustacean ACh receptors, appearing on an apparently inexcitable muscle, would have minimal voltage dependence. This appears to not be the case, although it is possible that under certain physiological conditions electrogenic capabilities may be induced in these muscles (Lingle, 1981).

#### *Comparison with Glutamate Excitatory Currents in Arthropods*

From the information obtained in this study it is now possible to compare the kinetic and conductance properties of excitatory currents activated by two different transmitters within the same phyla and within the same organism. This subject will be considered in more detail in the paper that follows (Lingle and Auerbach, 1983).

We would like to thank Dr. Marder and Dr. del Castillo, in whose laboratories the experiments were performed. The work was done while C.L. and A.A. were Muscular Dystrophy Post-Doctoral Fellows. We also thank Dr. P. Specht for PDP-12 assembly language programming. The work was supported by National Science Foundation grant BN578-15399 (to E. Marder) and U. S. Public Health Service grant NS07464 (to J. del Castillo).

*Received for publication 11 March 1982 and in revised form 14 December 1982.*

#### REFERENCES

- Adams, P. R. 1977. Relaxation experiments using bath-applied suberyldicholine. *J. Physiol. (Lond.)* 268:271-289.

- Adams, P. R. 1981. Acetylcholine receptor kinetics. *J. Membr. Biol.* 58:161-174.
- Adams, P. R., and B. Sakmann. 1978. A comparison of current-voltage relations for full and partial agonists. *J. Physiol. (Lond.)*. 283:621-644.
- Anderson, C. R., S. G. Cull-Candy, and R. Miledi. 1978. Glutamate current noise: post-synaptic channel kinetics investigated under voltage clamp. *J. Physiol. (Lond.)*. 282:219-242.
- Anderson, C. R., and C. F. Stevens. 1973. Voltage clamp analysis of acetylcholine produced end-plate current fluctuations at frog neuromuscular junction. *J. Physiol. (Lond.)*. 235:655-692.
- Ascher, P., W. A. Large, and H. P. Rang. 1979. Studies on the mechanism of action of acetylcholine antagonists on rat parasympathetic ganglion cells. *J. Physiol. (Lond.)*. 295:139-170.
- Ascher, P., A. Marty, and T. O. Neild. 1978. Life time and elementary conductance of the channels mediating the excitatory effects of acetylcholine in *Aplysia* neurones. *J. Physiol. (Lond.)*. 278:177-206.
- Brenner, H. R., and B. Sakmann. 1978. Gating properties of the acetylcholine receptor at newly formed neuromuscular synapses. *Nature (Lond.)*. 271:366-368.
- Colquhoun, D., and A. G. Hawkes. 1977. Relaxation and fluctuations of membrane currents that flow through drug-operated channels. *Proc. R. Soc. Lond. B Biol. Sci.* 199:231-262.
- Colquhoun, D., and A. G. Hawkes. 1981. On the stochastic properties of single ion channels. *Proc. R. Soc. Lond. B Biol. Sci.* 211:205-235.
- Colquhoun, D., and B. Sakmann. 1981. Fluctuations in the microsecond time range of the current through single acetylcholine receptor ion channels. *Nature (Lond.)*. 294:646-466.
- Crawford, A. C., and R. N. McBurney. 1976. On the elementary conductance event produced by L-glutamate and quanta of the natural transmitter at the neuromuscular junctions of *Maia squinado*. *J. Physiol. (Lond.)*. 258:205-225.
- Cull-Candy, S. G., R. Miledi, and I. Parker. 1981. Single glutamate-activated channels recorded from locust muscle fibres with perfused patch-clamp electrodes. *J. Physiol. (Lond.)*. 321:195-210.
- Cull-Candy, S. G., and I. Parker. 1982. Rapid kinetics of single glutamate-receptor channels. *Nature (Lond.)*. 295:410-412.
- del Castillo, J., and B. Katz. 1957. Interaction at end-plate receptors between different choline derivatives. *Proc. R. Soc. Lond. B Biol. Sci.* 146:369-381.
- Dionne, V. E., and R. L. Parsons. 1981. Characteristics of the acetylcholine-operated channel at the twitch and slow fibre neuromuscular junctions of the garter snake. *J. Physiol. (Lond.)*. 310:145-158.
- Dudel, J. 1974. Nonlinear voltage dependence of excitatory synaptic current in crayfish muscle. *Pflügers Arch. Eur. J. Physiol.* 352:227-241.
- Dudel, J. 1977. Voltage dependence of amplitude and time course of inhibitory synaptic current in crayfish muscle. *Pflügers Arch. Eur. J. Physiol.* 371:167-174.
- Dudel, J. 1978. Relaxation after a voltage step of inhibitory synaptic current elicited by nerve stimulation (crayfish neuromuscular junction). *Pflügers Arch. Eur. J. Physiol.* 376:151-157.
- Dudel, J., W. Finger, and H. Stettmeier. 1977. GABA-induced membrane current noise and the time course of the inhibitory synaptic current in crayfish muscle. *Neurosci. Lett.* 6:203-208.
- Dudel, J., and S. W. Kuffler. 1961. The quantal nature of transmission and spontaneous miniature potentials at the crayfish neuromuscular junction. *J. Physiol. (Lond.)*. 155:514-529.
- Faber, D. S., and H. Korn. 1980. Single-shot activation accounts for duration of inhibitory postsynaptic potentials in a central neuron. *Sciences (NY)*. 208:612-615.

- Finger, W., and H. Stettmeier. 1980. Efficacy of the two microelectrode voltage clamp technique in crayfish muscle. *Pflügers Arch. Eur. J. Physiol.* 387:133-141.
- Gardner, D. 1980. Membrane-potential effects on an inhibitory post-synaptic conductance in *Aplysia* buccal ganglia. *J. Physiol. (Lond.)*. 304:165-180.
- Gardner, D., and C. F. Stevens. 1980. Rate-limiting step of inhibitory post-synaptic current decay in *Aplysia* buccal ganglia. *J. Physiol. (Lond.)*. 304:145-164.
- Govind, C. K., H. L. Atwood, and D. M. Maynard. 1975. Innervation and neuromuscular physiology of intrinsic foregut muscle of the blue crab and spiny lobster. *J. Comp. Physiol.* 96:185-204.
- Katz, B., and R. Miledi. 1972. The statistical nature of the acetylcholine potential and its molecular components. *J. Physiol. (Lond.)*. 224:665-700.
- Kuba, K., and S. Nishi. 1979. Characteristics of fast excitatory postsynaptic currents in bullfrog sympathetic ganglion cells. *Pflügers Arch. Eur. J. Physiol.* 378:205-212.
- Lester, H. A., D. D. Koblin, and R. E. Sheridan. 1978. Role of voltage-sensitive receptors in nicotinic transmission. *Biophys. J.* 21:181-194.
- Lingle, C. 1980. The sensitivity of decapod foregut muscles to acetylcholine and glutamate. *J. Comp. Physiol.* 138:187-199.
- Lingle, C. 1981. The modulatory action of dopamine on crustacean foregut neuromuscular preparations. *J. Exp. Biol.* 94:285-300.
- Lingle, C., and A. Auerbach. 1980. Analysis of channels activated by acetylcholine and glutamate in crustacean muscle. *Neurosci. Abstracts.* 6:754.
- Lingle, C., and A. Auerbach. 1983. Comparison of excitatory currents activated by different transmitters on crustacean muscle. II. Glutamate-activated currents and comparison with acetylcholine currents present on the same muscle. *J. Gen. Physiol.* 81:571-588.
- Lingle, C., J. S. Eisen, and E. Marder. 1981. Block of glutamatergic excitatory synaptic channels by chlorisondamine. *Mol. Pharmacol.* 19:349-353.
- MacDermott, A. B., E. A. Connor, V. E. Dionne, and R. L. Parsons. 1980. Voltage-clamp study of fast excitatory synaptic currents in bullfrog sympathetic ganglion cells. *J. Gen. Physiol.* 75:39-60.
- Magleby, K. L., and C. F. Stevens. 1972. The effect of voltage on the time course of end-plate currents. *J. Physiol. (Lond.)*. 223:151-171.
- Marder, E. 1976. Cholinergic motor neurons in the stomatogastric system of the lobster. *J. Physiol. (Lond.)*. 257:63-86.
- Marder, E., and D. Paupardin-Tritsch. 1980. The pharmacological profile of the acetylcholine response of a crustacean muscle. *J. Exp. Biol.* 88:147-159.
- Michler, A., and B. Sakmann. 1980. Receptor stability and channel conversion in the subsynaptic membrane of the developing mammalian neuromuscular junction. *Dev. Biol.* 80:1-17.
- Neher, E., and B. Sakmann. 1976. Single-channel currents recorded from membrane of denervated frog muscle fibres. *Nature (Lond.)*. 260:799-802.
- Nelson, D. J., and F. Sachs. 1979. Single ionic channels observed in tissue-cultured muscle. *Nature (Lond.)*. 282:861-863.
- Onodera, A., and A. Takeuchi. 1975. Ionic mechanism of the excitatory synaptic membrane of the crayfish neuromuscular junction. *J. Physiol. (Lond.)*. 252:295-318.
- Onodera, A., and A. Takeuchi. 1978. Effects of membrane potential and temperature on the excitatory post-synaptic current in the crayfish muscle. *J. Physiol. (Lond.)*. 276:183-192.
- Rang, H. P. 1981. The characteristics of synaptic currents and responses to acetylcholine of rat submandibular ganglion cells. *J. Physiol. (Lond.)*. 311:23-55.

- Sakmann, B., and P. R. Adams. 1979. Biophysical aspects of agonist action at frog endplate. *Adv. Pharmacol. Ther.* 1:81-90.
- Schuetze, S. W. 1980. The acetylcholine channel open time in chick muscle is not decreased following innervation. *J. Physiol. (Lond.)*. 303:111-124.
- Schuetze, S. W., E. F. Frank, and G. D. Fischbach. 1978. Channel open time and metabolic stability of synaptic and extrasynaptic acetylcholine receptors on cultured chick myotubes. *Proc. Natl. Acad. Sci. USA*. 75:520-523.
- Sheridan, R. E. 1976. Voltage-independent acetylcholine receptors in the skate electroplaque. *Biophys. J.* 16:212a. (Abstr.)
- Steinbach, J. H. 1980. Activation of nicotinic acetylcholine receptors. *In* The Cell Surface and Neuronal Function. C. W. Cotman, G. Poste, and G. L. Nicolson, editors. Elsevier/North-Holland Biomedical Press, New York. 119-156.